

Harvest Energy from the Water: A Self-Sustained Wireless Water Quality Sensing System

QI CHEN, Montana State University

YE LIU, Southeast University

GUANGCHI LIU and QING YANG, Montana State University

XIANMING SHI, Washington State University

HONGWEI GAO, Montana State University

LU SU, State University of New York at Buffalo

QUANLONG LI, Harbin Institute of Technology

Water quality data is incredibly important and valuable, but its acquisition is not always trivial. A promising solution is to distribute a wireless sensor network in water to measure and collect the data; however, a drawback exists in that the batteries of the system must be replaced or recharged after being exhausted. To mitigate this issue, we designed a self-sustained water quality sensing system that is powered by renewable bioenergy generated from microbial fuel cells (MFCs). MFCs collect the energy released from native magnesium oxidizing microorganisms (MOMs) that are abundant in natural waters. The proposed energy-harvesting technology is environmentally friendly and can provide maintenance-free power to sensors for several years. Despite these benefits, an MFC can only provide microwatt-level power that is not sufficient to continuously power a sensor. To address this issue, we designed a power management module to accumulate energy when the input voltage is as low as 0.33V. We also proposed a radio-frequency (RF) activation technique to remotely activate sensors that otherwise are switched off in default. With this innovative technique, a sensor's energy consumption in sleep mode can be completely avoided. Additionally, this design can enable on-demand data acquisitions from sensors. We implement the proposed system and evaluate its performance in a stream. In 3-month field experiments, we find the system is able to reliably collect water quality data and is robust to environment changes.

CCS Concepts: • **General and reference** → **Experimentation**; • **Networks** → **Network experimentation**; • **Computer systems organization** → **Sensor networks**; • **Hardware** → PCB design and layout;

Additional Key Words and Phrases: Energy harvesting, microbial fuel cell, power management, radio-frequency (RF) activation, water quality monitoring

Authors' addresses: Q. Chen, G. Liu, and Q. Yang, Gianforte School of Computing, Montana State University, Bozeman, MT, USA 59717; emails: {qi.chen2, guangchi.liu}@msu.montana.edu, qing.yang@montana.edu; Y. Liu, National ASIC System Engineering Research Center, Southeast University, Nanjing, Jiangsu, P.R. China 210096; email: liuyefancy@seu.edu.cn; X. Shi, Civil and Environmental Engineering Department, Washington State University, Pullman, WA, USA 99164; email: xianming.shi@wsu.edu; H. Gao, Electrical and Computer Engineering Department, Montana State University, Bozeman, MT, USA 59717; email: hgao@ece.montana.edu; L. Su, Computer Science and Engineering Department, State University of New York at Buffalo, Buffalo, NY 14260; email: lusu@buffalo.edu; Q. Li, School of Commuter Science and Technology, Harbin Institute of Technology, Harbin, Heilongjiang, P.R. China 150001; email: liquanlong@hit.edu.cn.

Permission to make digital or hard copies of all or part of this work for personal or classroom use is granted without fee provided that copies are not made or distributed for profit or commercial advantage and that copies bear this notice and the full citation on the first page. Copyrights for components of this work owned by others than ACM must be honored. Abstracting with credit is permitted. To copy otherwise, or republish, to post on servers or to redistribute to lists, requires prior specific permission and/or a fee. Request permissions from permissions@acm.org.

© 2017 ACM 1539-9087/2017/09-ART3 \$15.00

<https://doi.org/10.1145/3047646>

ACM Reference format:

Qi Chen, Ye Liu, Guangchi Liu, Qing Yang, Xianming Shi, Hongwei Gao, Lu Su, and Quanlong Li. 2017. Harvest Energy from the Water: A Self-Sustained Wireless Water Quality Sensing System. *ACM Trans. Embed. Comput. Syst.* 17, 1, Article 3 (September 2017), 24 pages.
<https://doi.org/10.1145/3047646>

1 INTRODUCTION

1.1 Motivation

Water affects every aspect of our lives (e.g., drinking supplies, agriculture production, factory operation, and recreation). Water quality monitoring is extremely important to our health and well-being, and it helps us prevent pollution in our waterways, assists farmers to better manage land and crops, and supports local, state, and national governments to efficiently monitor water supplies.

As important as water quality monitoring data is, it isn't easy to measure. There are currently three types of solutions to water quality monitoring. The first approach is to manually collect water samples and conduct chemical analysis in laboratories. Another approach is to use a flow-through monitoring station to pump water to the sensors in a permanent shelter. A more attractive approach, especially for remote or inaccessible locations, is to place the sensors in situ (immersed directly into the water). However, batteries in the system need to be replaced after being exhausted. Replacing batteries for an array of sensors not only is time- and labor-intensive but also makes the system susceptible to missing events that occur during this gap. Therefore, it is essential to design a self-sustained sensing system to realize a long-term and wide-area multiparameter monitoring of water quality.

1.2 Proposed Approach

A promising solution to the problem of finite battery lifetime is the use of energy-harvesting techniques. Energy harvesting refers to scavenging energy from ambient environments or other energy sources and converting it to electrical energy (Sudevalayam and Kulkarni 2011). Among renewable energy sources, solar energy is by far the largest exploitable resource. Harvesting solar energy in water, however, is challenging due to the difficulty of installing and floating solar panels on the surface of water. It is also possible to harvest mechanical energy from water waves to power sensors (Pobering and Schwesinger 2008). This technique requires continuous movements of water, which might be absent in ponds and lakes. Unlike existing techniques, we propose using an innovative microbial fuel cell (MFC)-based energy-harvesting solution.

MFCs are devices that convert chemical energy to electrical energy using microorganisms (or bacteria) as the catalysts (Logan et al. 2006). Electrons produced by the bacteria are transferred to the negative terminal (anode) and flow to the positive terminal (cathode). Opposite to the direction that electrons flow, a positive current goes from the positive to negative terminals. These two terminals are connected through a wire as a conductive bridge. By replacing that wire with a sensor, an MFC-powered sensor network is constructed. Because bacteria can survive for a very long period of time, well beyond the lifetimes of electronic devices, MFCs are considered a strong and reliable energy source. While MFCs tend to produce less energy than commercial fuel cells, they are able to generate power at the ambient temperature and harvest energy from the water. Compared to other solutions, MFCs do not require water movements or sunlight, so they can be applied in natural waters including creeks, rivers, ponds, and lakes.

Due to the fluctuation of energy generated from MFCs, we designed a power management system to regulate the power and offer a stable DC voltage. That DC voltage is used to power sensors

that automatically measure the temperature, pH, and level of dissolved oxygen in the water. It then periodically transmits collected data to a landbased gateway node. The gateway node then forwards the data to a remote data center via cellular networks. Relative to current practice, the proposed system provides a self-sustained and maintenance-free power supply that greatly reduces the need for changing/charging batteries periodically.

1.3 Technical Challenges and Solutions

Using MFCs as a maintenance-free power source for sensors in a water quality monitoring system is a challenging and unexplored problem. The key technical challenge is how to efficiently harvest bioenergy from bacteria in the water. Unlike traditional MFCs that utilize a bioanode and tend to have limited scalability and low energy generation, our MFC design features a biocathode coupled with a sacrificial anode. When there are little microbial activities, it is in essence a battery; when there are significant microbial activities, it becomes an MFC.

Another technical challenge is the conflict between the ultra-low power generated from MFCs and the (two orders of magnitude) higher power requirement of sensors. The typical output from MFCs is about 0.33V and 400 μ W, which is not enough to constantly power a sensor and its communication module. To address this challenge, we designed a power management circuit to store energy in three supercapacitors connected in parallel. These supercapacitors are then connected in series to provide a 1V stable power to a booster.

The next technical challenge is that a sensor is completely off when there is not enough energy provided by an MFC. In this case, the three supercapacitors will be in charging mode and no power will be output to the sensor. Essentially, a sensor is turned on and off periodically. This period is determined by the energy generation rate of MFCs, so it is unpredictable and thus traditional duty-cycle approaches (Jiang et al. 2005; Gu and He 2007) are not feasible.

The last technical challenge is how to keep a low energy consumption on the gateway node. Because the gateway node does not know when a sensor starts to work, it will be always awake and ready to receive data. The last two challenges can be addressed by the remote radio-frequency (RF) activation technique, which enables the gateway to pull data from sensors in an on-demand manner. With this innovative technique, sensors are woken up only when they receive an activation signal from the gateway. Without the activation signal, a sensor is completely off and its MFC accumulates energy. As such, the gateway is able to control when a sensor starts to sense and transmit data.

1.4 Key Contributions

In this article, we make the following key contributions:

- We designed an in situ water quality monitoring system based on renewable and self-sustaining bioenergy generated from MFCs. As such, sensors in the system can operate continuously for years, without the need for recharging or replacing their batteries.
- We designed and fabricated a power management module that is able to achieve high energy conversion efficiency even when the MFC voltage is as low as 0.33V.
- We implemented a remote RF activation technique that enables on-demand data acquisition from sensors. This technique not only reduces the energy consumption on the gateway but also enables adjustable working periods on a sensor.
- We implemented and evaluated the proposed system in a real-world setting. From field experiments that last for several months, we find that the proposed system is effective and robust.

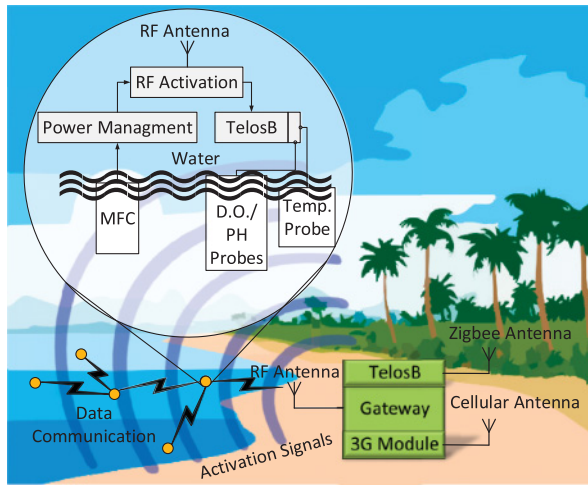


Fig. 1. Architecture of the self-sustained water quality monitoring system.

The rest of this article is organized as follows. In Section 2, we introduce the overview of the proposed water quality monitoring system. In Section 3, we investigate the power performance of the fabricated MFC. In Section 4, we explain how to manage the ultra-low energy generated from MFCs. In Section 5, we describe the technique of using RF signals to remotely activate sensors. In Section 6, we evaluate the proposed sensing system. In Section 7, we summarize the related work. The conclusion is given in Section 8.

2 SYSTEM OVERVIEW

An overview of the proposed system is presented in Figure 1. The proposed system consists of sensors deployed in water to monitor water quality, and gateway nodes to collect sensing data. A sensor consists of an MFC, a power management and RF activation module, a TelosB mote, and several sensing probes. MFCs harvest energy from water and output the energy to the power management module. Sensors are then powered on as long as the RF activation module in the power management circuit is activated by RF signals. The temperature, dissolved oxygen (DO), and pH sensing probes are connected to the TelosB mote. All sensing probes and the MFC are immersed in the water, but the sensor itself floats on the water. In fact, the sensor and its power management module could be in water as long as the wireless antennas are above the water. The gateway node uses a host device to control the TelosB mote (MEMSIC 2015). It will send RF signals to activate sensors and then collect the sensing data. The data is then forwarded via a 3G cellular module to a remote data center. In practice, the gateway node adopts 540MHz radios to activate the sensors. The spectrum is located in the TV band and widely used in RF energy-harvesting applications (Xiao et al. 2015). In addition, this frequency will not cause interference to the Zigbee communications between sensors. Although the current system contains a few sensors, it can be extended to a large-scale sensing platform and then form an Internet of Things system (Al-Fuqaha et al. 2015).

2.1 Microbial Fuel Cells

MFCs harness the native population of manganese-oxidizing microorganisms (MOMs) abundant in natural waters and use microbial metabolism to convert biochemical energy to electrical

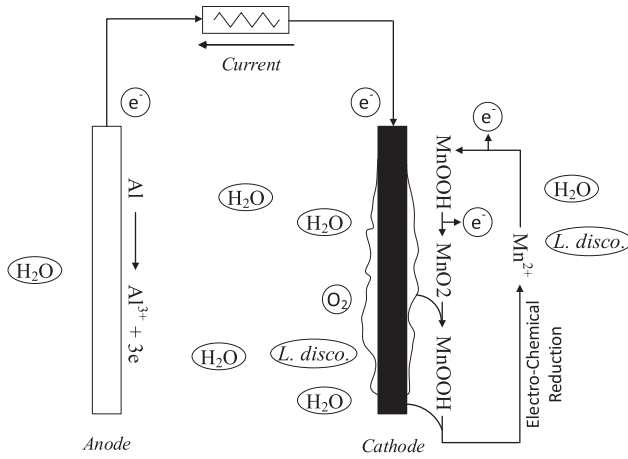
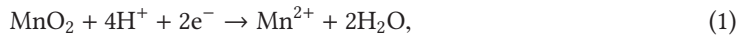


Fig. 2. Schematic of the MFC consisting of a sacrificial anode of aluminum alloy and a cathode of porous graphite covered by manganese dioxide (Nguyen et al. 2007).

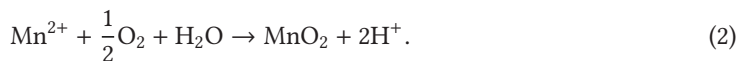
energy. Manganese (Mn) is Earth’s second-most abundant transition metal (the first one is iron). Soluble Mn(II) in natural waters can reach up to millimolar concentrations, so it becomes the dominant mechanism of oxidizing Mn(II) to insoluble Mn(III, IV) oxides in freshwater. As a result, manganese-oxidizing microorganisms are ubiquitous in waters and play a critical role in the biogeochemical cycling of manganese, iron, nitrogen, and carbon (Tebo et al. 2005). The MOM used in our MFC is called *Leptothrix discophora* SP-6. We select the *Leptothrix discophora* SP-6 bacteria because (1) they are abundant in waters and (2) they survive in cold temperatures or even some relatively harsh conditions.

MFCs consist of two chamber systems: the anodic chamber of aluminum alloy and the cathodic chamber covered by manganese dioxide. As shown in Figure 2, the anode and cathode compartments are separated by an ion-exchange membrane that moves ions in one direction and prevents the passage of water. In the cathodic chamber, the following electrochemical reaction takes place:



where an Mn(IV) oxide is converted to an Mn(II) oxidation. Two electrons released from the anodic chamber are absorbed in this reaction. Because electrons move from the anodic chamber to the cathodic chamber, a current is generated from the cathode to the anode. The current is then used to charge the supercapacitors in the power management module.

If the previous reaction continues without supplying additional MnO_2 , the cathodic chamber will eventually run out of Mn(IV) oxide and the MFC will not generate any electricity. To make the MFC self-sustained, the *Leptothrix discophora* SP-6 bacteria are introduced to help to convert Mn(II) oxidation to Mn(IV) oxide in the following oxygen reduction reaction:



Apparently, the active levels of the bacteria in the cathodic chamber determine the speed of the aforementioned reaction. If the bacteria are active and provided enough nutrients, the reactions in Equations (1) and (2) will continue occurring. That also means the MFC will keep generating energy.

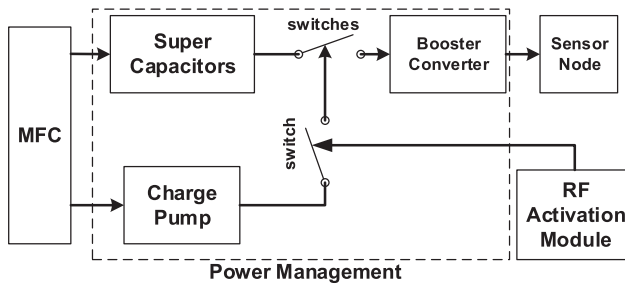


Fig. 3. Schematic of the power management module. The MFC charges the supercapacitors and charge pump simultaneously. When the charge pump is fully charged and RF activation signals are received, all switches are closed so that energy is output to the booster converter that increases the power's voltage from 1.8V to 3.0V.

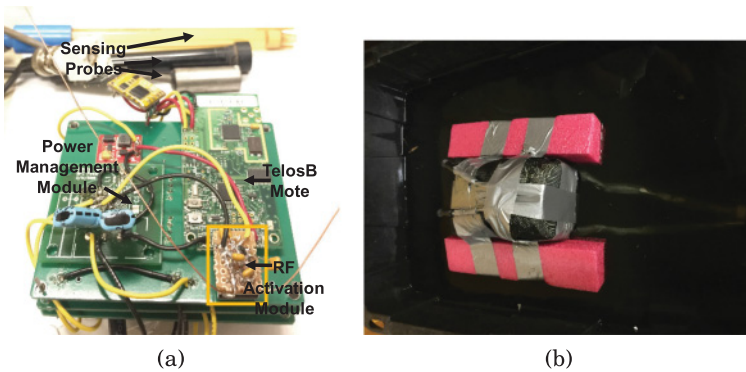


Fig. 4. (a) The fabricated power management circuit is connected to a TelosB node and two sensing probes. (b) A sensor floats on the water with its sensing probes immersed in the water.

2.2 Power Management

The major functionality of the power management module is to bridge the voltage and current gaps between an MFC and a sensor (including the attached sensing probes). It provides high enough voltage and current for the sensor using the ultra-low voltage and current generated from the MFC. To accomplish this goal, the module collects low power from the MFC over a relatively long period and releases high enough power to the sensor in a short period of time.

As shown in Figure 3, the power management module consists of supercapacitors, a charge pump chip, a booster converter, switches, and an RF activation module. Note that our solution is different from traditional power management circuits that use charge pumps to store energy (Meehan et al. 2011). We use a charge pump to control only a set of switches, which reduces the time needed for the charge pump to be fully charged. The proposed power management module can work with an input voltage as low as 0.33V.

Another important component in this design is the RF activation module. It enables the gateway node to control when and how long a sensor will collect and transmit sensing data. After this module harvests enough energy from the activation RF signals sent from the gateway, it will close the switch between the power management module and the sensor. As such, the sensor will be powered on until the gateway stops sending these activation signals. The fabricated power management module, RF activation module, and TelosB node are connected, as shown in Figure 4(a).

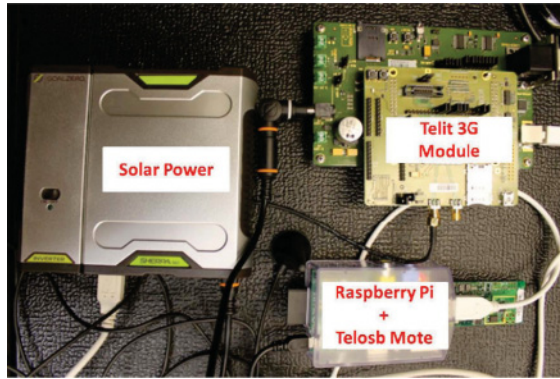


Fig. 5. Prototype of the gateway node.

2.3 Sensor

We adopt the TelosB mote as the main sensor node. Three types of sensing probes are connected to the sensor node. These sensing probes will measure the temperature, DO, and pH of the water being monitored. The AtlasScientific temperature sensor is connected to the TelosB through an analog-to-digital converter (ADC). The AtlasScientific dissolved oxygen sensor and AtlasScientific pH sensor are connected to the TelosB via serial ports (UART1). We select these sensing probes mainly because of their outstanding performance in long-term field experiments. To obtain accurate sensing data from the DO (or pH) sensing probe(s), an embedded processing circuit (e.g., the AtlasScientific EZO class DO circuit) is needed. This circuit usually draws hundreds of *mW* energy to convert the raw data read from a DO probe to accurate DO concentration measurements. Therefore, it consumes more energy to read DO (or pH) data than temperature data.

Because a TelosB node only provides one UART1 port, either an oxygen or a pH sensor is installed on one TelosB. When a TelosB is activated, it starts to collect data from its ADC and UART ports for 500ms. This time period is chosen because we find the readings from sensing probes are stabilized within this time period. After that, the data are sent to the gateway via the collection tree protocol (Gnawali et al. 2009). We choose BoX-MAC (Moss and Levis 2008) as the default MAC protocol. To ensure a TelosB works well in the water, it is placed in a plastic enclosure. The gaps on the enclosure are sealed by marine epoxy, a permanent, waterproof adhesive. Foams are attached to the enclosure to float a sensor on the water's surface, as shown in Figure 4(b).

2.4 Gateway

The gateway node is designed to pull water quality information (e.g., temperature, DO, pH data) from sensors. Figure 5 shows the prototype of the gateway where the host device (Raspberry Pi) is connected to two slave devices (TelosB and Telit 3G wireless module). The TelosB node receives messages from the sensor network and sends them to a remote data management center via the 3G wireless module. To protect the sensing data, the data management center could be hosted on a cloud server with security protection schemes enabled (Fu et al. 2016b; Zhangjie et al. 2015). We adopt an Agilent N5182A signal generator to send 540MHz RF signals to remotely activate sensors. To realize a self-sustained sensing system, the gateway is powered by two 20W solar panels with a rechargeable battery.

From field tests, we find that harvested solar energy on the gateway nodes changes tremendously with different weather conditions. When it encounters two continuous cloudy or raining



Fig. 6. (a) MFC's anode electrically connected to a copper wire. (b) MFC's cathode without the biofilm grown on it. (c) The cathode fixed by three polycarbonate sheets. (d) Assembled MFC wrapped by two rubber gaskets to prevent mechanical damages.

days, the harvested energy is insufficient to power the gateway node. On the other hand, water quality information is more valuable when the weather condition changes. To solve this problem, the gateway node works in a duty-cycle manner; that is, it periodically sends RF signals to activate sensors and pull data from them. At other times, it is in sleeping mode to save energy.

3 MICROBIAL FUEL CELLS

In this section, we will introduce the prototype of MFCs fabricated in our lab, followed by a power density analysis of the MFCs.

3.1 Prototype of MFC

To improve the power generation of MFCs, we significantly reduce the distance between the cathode and anode to 5mm , so as to reduce the internal resistance of the MFC. We also increase the electrode dimensions (i.e., each cathode with exposed surface area of approximately 386 square inches). The increased surface of the cathode enhances the biocathode's performance by lowering its activation overpotential. Moreover, a variety of surface treatments are employed on the biocathode to reduce the internal resistance of MFCs. For example, we use the porous membrane to separate the biocathode compartment and the external aqueous environment.

In Figure 6, we can see that the MFC's anode is made of an aluminum alloy plate measuring $0.5 \times 6 \times 12$ inches and weighing approximately 4 pounds. The MFC cathode is made by a composite material, and it has about the same size as the anode but weighs approximately 14 pounds. The cathode is cultured in room temperature for 15 days to allow bacteria to grow on it. The culture solution is replaced with new midexponential phase culture every day to ensure that the bacteria in the plastic box remained in the exponential growth phase. The MFC is then assembled using a polycarbonate sheet and shower pan liner. The anode and cathode compartments are then wrapped by a shower pan liner and fixed with a polycarbonate sheet. On the polycarbonate sheet, we drill multiple $3/8$ -inch holes to allow water to go in and out of the MFC.

3.2 Power Density of MFC

We simulate four different environmental scenarios to test the MFC's power density. For each environmental scenario, we test the MFC's output current and power density measured by the mW/m^2 . In the calculation, we use 0.249m^2 as the surface area of the MFC. All the measurements are taken at least 30 minutes after changing the environmental condition. Overall, the power density of the MFC first increases as the current increases. After the power density reaches the maximum point, it decreases as the current further increases. In summary, the environmental parameters including pH, temperature, dissolved oxygen concentration, and chloride concentration would affect the power output of the MFC.

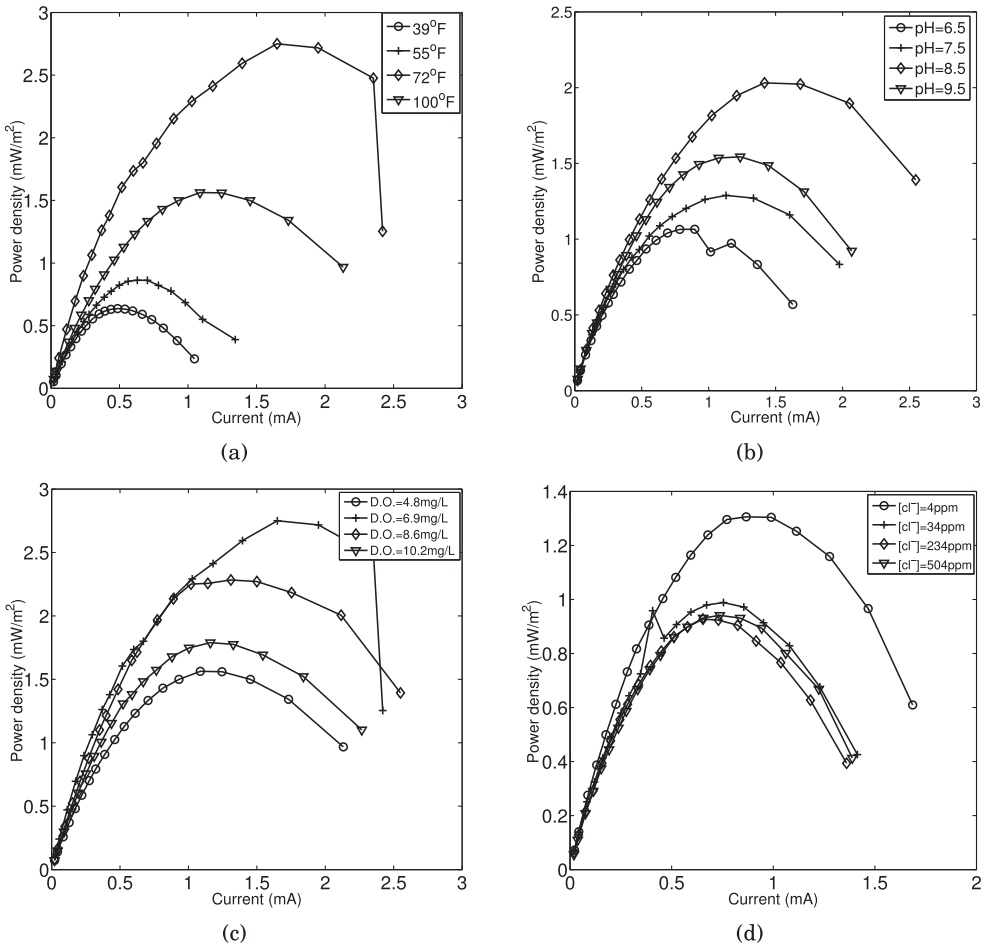


Fig. 7. Power density of the MFC under different temperatures (a), pH (b), dissolved oxygen (c), and chloride (d) concentrations.

Water temperature is an important factor for the growth and aging of MOM, biofilm attachment/detachment, and biomineralization processes. As shown in Figure 7(a), the results indicate that the water temperature of 72°F provides the best environmental condition for the biocathode MFC to produce a relatively high maximum power density (2.8 mW/m²). In contrast, the water temperature of 39°F corresponds to the worst environmental condition for the biocathode MFC (0.6 mW/m²).

The proper pH for bacterial growth should provide chemically stable and nontoxic conditions without interfering with biochemical reactions. In Figure 7(b), results indicate that when the water pH is 8.5, the MFC produces a relatively high maximum power density. Increasing the level of DO generally increases the power output of the MFC. As shown in Figure 7(c), a DO of 6.9 mg/L corresponds to the highest maximum power density and a DO of 4.8 mg/L to the worst performance. The decrease of DO from 10.2 mg/L to 6.9 mg/L, however, corresponds to the increase in the MFC power density. This is likely attributable to the decrease in flow rate from 11.77 L/min to 0 L/min and thus less dilution of nutrients. It will overshadow the beneficial effect of increasing DO on the metabolism of the MOM biofilm.

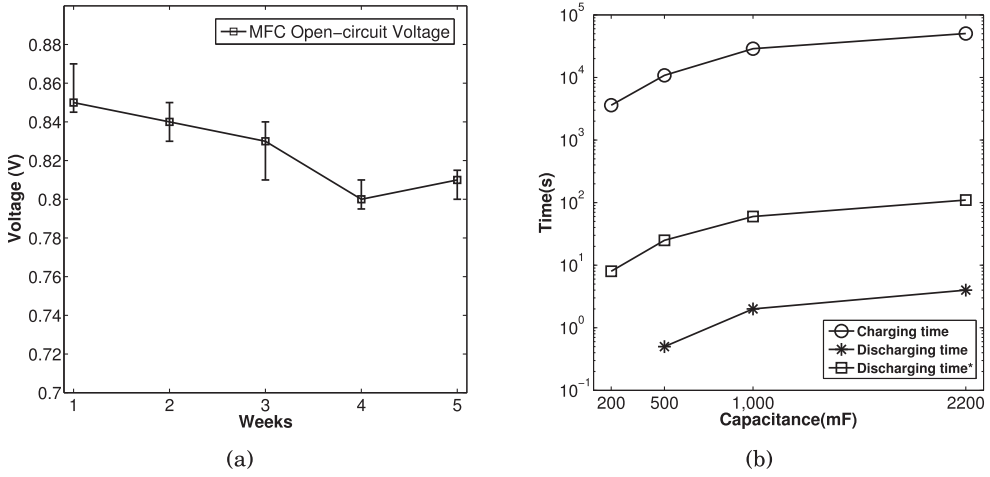


Fig. 8. (a) Measured open-circuit voltages of MFC from September 5, 2014, to October 10, 2014. (b) Charging and discharging times of the charge pumps in the traditional and proposed power management systems.

On the one hand, the increase in chloride concentration greatly reduces the internal resistance of the MFC and thus improves its power output. On the other hand, the increase in chloride concentration also negatively impacts the growth and biomineralization process of *Leptothrix discophora* SP-6 (a freshwater MOM), thus reducing the power output of the MFC. As observed in Figure 7(d), the results indicate that the [Cl⁻] of 4ppm corresponds to the highest maximum power density. In contrast, the [Cl⁻] of 234ppm and 504ppm provide the worst environmental conditions for the biocathode MFC.

3.3 Field Tests of MFC

We then deploy the MFC into a local stream. At the moment when the MFC is placed in the stream, the water has a measured dissolved oxygen concentration of 9.07 parts per million (ppm) and pH of 8.0. The temperature of the stream is 60°F; the temperature of the water in the fuel cell is 63.5°F. From field tests, we find the maximum output power is 0.4mW when the MFC's output voltage is 0.33V and current is 1.2mA. To output a 0.5V power, the harvested energy from MFC reduces to 0.3mW with a current of 0.6mA. The low power density of MFC is mainly caused by its large internal resistance, which is usually a few hundreds of Ohms. Due to the high electrical resistivity of fresh waters, it is extremely difficult to reduce MFC's internal resistance as it must be immersed in the water. We conclude that the amount of energy generated by MFC is far from sufficient to continuously power any commercial off-the-shelf (COTS) sensor.

The MFC is then left in the stream, unconnected, for 5 weeks. We evaluate its long-term performance by measuring its open-circuit voltages three times per day. As shown in Figure 8(a), the output voltage of MFCs gradually decreases from 0.85V to 0.8V and stays stable afterward. The fluctuation of open-circuit voltages in each week is simply caused by the environmental changes of the stream. Note that when an external load is connected, the MFC's output voltage will decrease to around 0.33V.

4 POWER MANAGEMENT

Although the MFC is a self-sustained power source, it provides an ultra-low energy output that is not able to constantly power a sensor and attached sensing devices. Power consumption of a TelosB

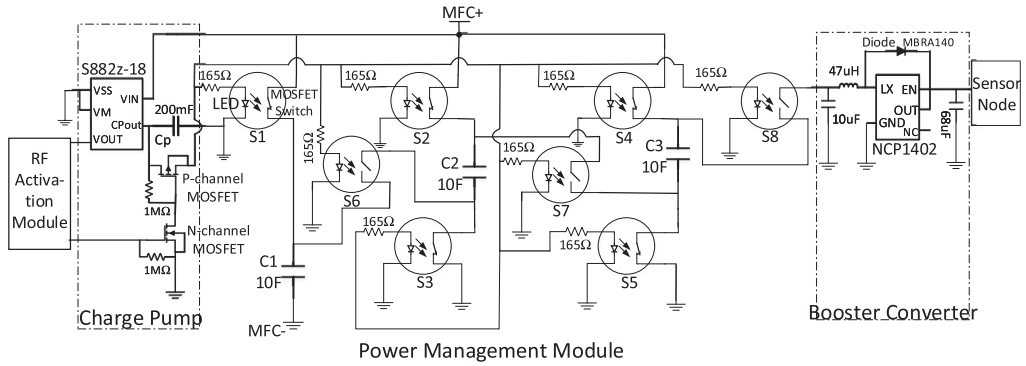


Fig. 9. In the power management module, switches S1 – S5 are closed by default so that supercapacitors C1 – C3 are charged in parallel. After the charge pump is fully charged, it discharges to open S1 – S5 and close S6 – S8 so that C1 – C3 are connected in series to output a 1V power. It is then converted to a 3.3V power by the booster converter.

sensor is usually hundreds of microwatts with a voltage of 3.3V. Traditional power management solutions cannot efficiently handle the tiny power supplied by MFCs (Pughat and Sharma 2016). Therefore, it is essential to design a power management circuit to accumulate energy generated from MFCs and power-connected sensors when enough energy is collected.

The detailed design of our power management module is shown in Figure 9. In the figure, the solid-state relay switches S1 – S5 are closed by default, so the 10F supercapacitors C1 – C3 are charged in parallel by an MFC. The switches S1 – S5 are then controlled by a charge pump that consists of a control chip (e.g., Seiko S-882Z) and a 200mF supercapacitor C_p . The C_p draws currents from the MFC and increases its voltage until a certain threshold (e.g., 1.8V or 2.4V) is reached. The control chip is then in the discharging mode; that is, it will open S1 – S5 and close S6 – S8. As such, supercapacitors C1 – C3 are connected in series and the output voltage reaches 1V, which is enough to drive a booster converter. The booster converter will convert the input power from 1V to stable 3.3V. When the charge pump stops discharging, the switches go back to the default configuration where C1 – C3 are connected in parallel and switches S1 – S5 are closed and S6 – S8 are open.

We adopt three supercapacitors in the design because the MFC reaches its maximum output power when its voltage is 0.33V. When three supercapacitors are completely charged and connected in series, their power voltage will reach 1V. The number of supercapacitors in our design can be adjusted based on the characteristics of the power supply. Traditionally, a charge pump is used to accumulate energy to drive a sensor from an ambient power source. Unfortunately, most energy is lost in the conversion process on a charge pump. In our design, because the supercapacitors are directly charged by an MFC, the energy conversion efficiency is significantly improved.

We compare the discharging times of the proposed power management module and a typical charge pump, that is, a Seiko S-882Z with a supercapacitor C_p . The same charge pump is also used to control the switches in our module. To shorten the charging time, we adopt a stable 1V DC power supply. As shown in Figure 8(b), when $C_p = 200mF$, it takes the charge pump about an hour to be fully charged and its discharging time is only 8 seconds. When C_p increases, the charging and discharging times increase accordingly. The discharging time of our power management module (labeled as Discharging time*), however, is always at least one order of magnitude larger than that of a charge pump. This is mainly because the energy collected by a charge pump is used to control switches rather than to power a sensor.

Choosing an appropriate value of C_p requires that the discharging time be long enough for a sensor to finish assigned sensing and communication tasks. In other words, the charge pump needs to control switches $S_1 - S_8$ for a certain period of time. A large C_p can be used for a system that requires a low data rate but large data size. If frequent monitoring is needed, a small C_p might be a good choice. In summary, the capacitance of C_p can be adjusted in practice to achieve a desired data rate.

5 REMOTE ACTIVATION

To make efficient use of the tiny amount of energy harvested from an MFC, a sensor needs to be in the complete off mode rather than the sleeping mode, if there is no sensing task. When the sensor receives an RF activation signal from the gateway node, it is turned on and starts to sense and transmit water quality data.

5.1 Energy Consumption in Sleeping Mode

The duty cycle technique is widely applied in wireless sensor networks where sensors become active briefly and are kept in sleep mode for most of the time (He et al. 2012). Duty cycle is defined as the percentage of time a sensor is active in the whole operational time. For example, a 0.27% duty cycle usually means a sensor works for 10s per hour. Because an MFC only provides energy on the order of microwatts, it is impossible to implement even a 0.27% duty cycle in our system. This is because sensors still draw energy in sleeping mode. For example, the current draw by a TelosB node in sleeping mode is around $20\mu A$. If we use an MFC to power a TelosB node (with a 0.27% duty cycle), the residual energy of this node will be $-128.6J$ after 100 days. Here we ignore the start-up power consumption of a TelosB node. When a TelosB node is turned on, it first enters the sleep mode (current draw is $20\mu A$) for at most $860\mu s$ and then turns into the active mode. Compared to the energy consumption of wireless transmissions, this tiny amount of energy is ignored in our computation.

If a sensor is completely turned off when there is no sensing task, the energy consumption in sleeping mode can be eliminated. For example, the residual energy of a TelosB node will be $441.6J$ after 100 days, if it is turned off instead of being placed in sleeping mode. Here, we propose an innovative way to turn on a sensor (without human interruption) when it needs to sense, which will be introduced later.

5.2 RF Activation

As shown in Figure 10, we place an RF activation module between the supercapacitors and the booster converter. This module connects an MFC to a sensor by controlling a MOSFET switch when enough energy is harvested from received RF signals. In Figure 10, V_{in} indicates the rectified power voltage of a received RF signal. It then charges the Seiko S-882Z chip. When it is charged to 1.8V, the Seiko S-882Z will continuously output energy to close the MOSFET switch until V_{out} drops to 0.8V. As long as the RF signal is available, the MOSFET switch will be closed because the Seiko S-882Z chip is kept charged.

The proposed activation technology is particularly effective in a dense sensor network where a small region is monitored by a large amount of sensors. More gateway nodes need to be deployed in a large-scale network, due to the limited activation range of RF signals. The gateway node can choose to activate sensors on a predefined schedule or on demand. For example, the gateway node may periodically send RF signals to pull sensing data from sensors. It can also activate sensors only when a certain condition is satisfied (e.g., it starts to rain). The weather information can be obtained from external resources (e.g., National Oceanic and Atmospheric Administration (NOAA)) or measured by internal sensors on the gateway.

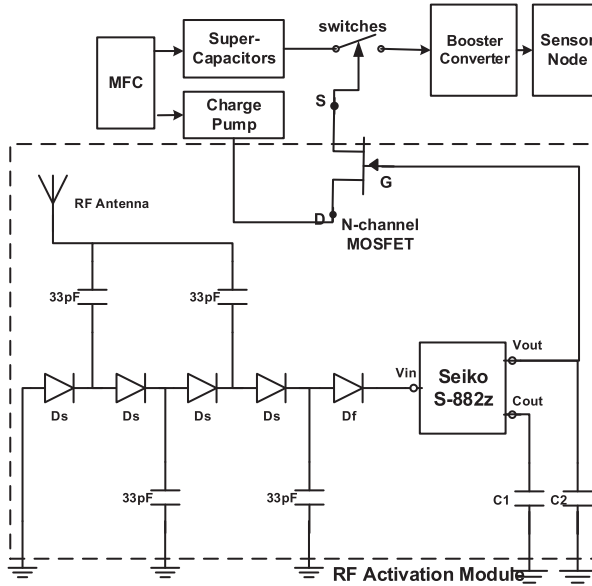


Fig. 10. In the RF activation module, the energy harvested from RF signals is first rectified and then used to charge capacitor C1 through the Seiko S-882Z chip. It starts discharging when C1 is charged to 1.8V, so the MOSFET switch is closed to connect the MFC and the sensor.

Based on the free-space path loss model (Rappaport 1996), the power of received RF signals on a sensor can be expressed as

$$P_r = \frac{G_r G_t P_t}{\left(\frac{4\pi d}{\lambda}\right)^2}, \tag{3}$$

where P_t is the transmission power; G_r and G_t are the transmitting and receiving antenna gains, respectively; λ is the wavelength of the RF signal; and d is the distance between the transmitter and receiver. To increase the activation distance d , a low-frequency RF signal (e.g., 540MHz) is adopted in the proposed system. A high-gain directional antenna may also help to achieve a longer activation distance.

It is worthwhile to mention that a remote activation technique is important to energy-harvesting sensor networks with ultra-low power supplies. For example, after a sensor collects enough energy, it starts to transmit data to another node. However, the receiving node may be inactive due to insufficient energy harvested from ambient sources. Since the sender does not know whether its data is dropped due to weak channel conditions, packet collisions, or insufficient energy on the receiver, it will re-transmit the data until the maximum number of retransmissions is reached. Such asynchronized communication not only wastes the precious energy harvested on sensors but also increases the communication delay if traditional multihop routing protocols in sensor networks are adopted (Thulasiraman and White 2016).

6 FIELD EXPERIMENTS

We evaluate the performance of each component in the power management module. As shown in Figure 11, the entire sensing system including an MFC, a power management module, a temperature sensor, and a DO sensor is deployed in a local stream. To accurately record instantaneous

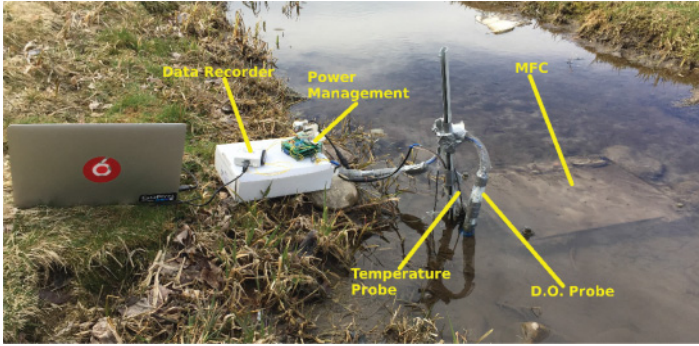


Fig. 11. All electronic components in the sensor are powered by the MFC that is placed in a local stream. The instantaneous voltage and current of each electronic component are measured by the NI USB6009 data recorder. Temperature and DO data are collected by the gateway node that is 10m away from the sensor.

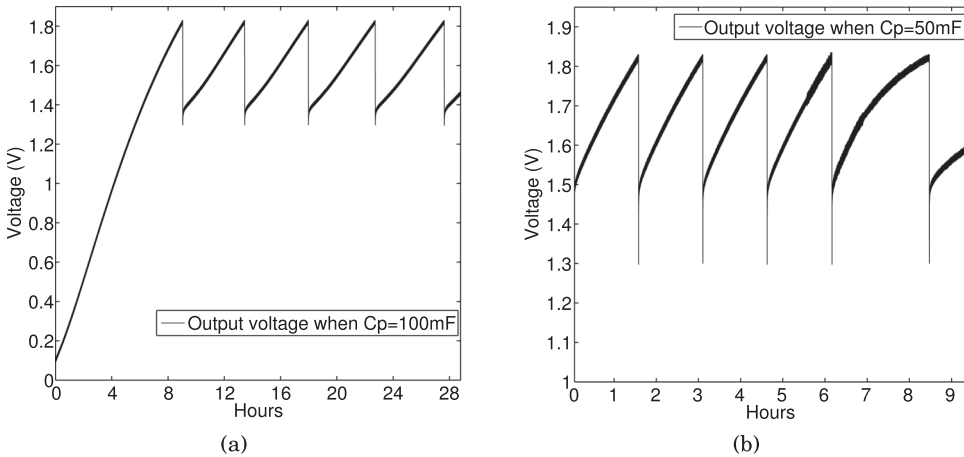


Fig. 12. Instantaneous voltages of the charge pumps with different C_p s.

voltages and currents, we use an NI (National Instruments) USB6009 data recorder that is connected to a laptop.

Insights: MFCs are proven to be a promising solution to harvesting energy from water, which leverages bacteria in water to oxidize organic molecules and release electrons (Logan et al. 2006). It is well known that MFCs can generate electricity using bacteria to break down organic substrates (Du et al. 2007b). It is worth mentioning that, at the moment of writing this article, our MFCs have been placed in a local stream for more than 18 months and the open-circuit voltage is still 0.95V. This implies the bacteria on the MFCs are still active, even after a cold winter season.

6.1 Power Management Module

In the experiment, we use two supercapacitors $C_p = 50mF$ and $C_p = 100mF$ on the charge pump. Figure 12(a) shows the charge pump's instantaneous voltages over a 28-hour period. The charge pump's voltage starts to increase from the first hour. At the same time, the MFC starts to charge the three parallel-connected supercapacitors $C_1 - C_3$. After the eighth hour, the charge pump's voltage reaches 1.8V; it starts to discharge and closes the switches $S_6 - S_8$, so the supercapacitors

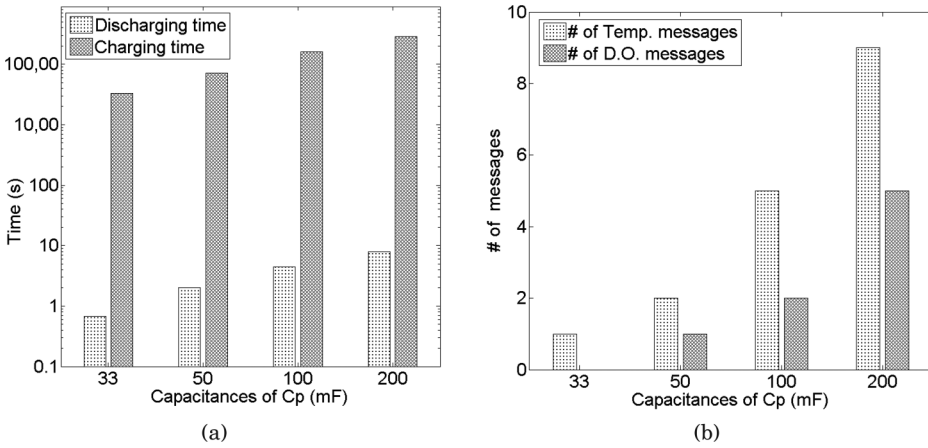


Fig. 13. (a) Charging and discharging times of the charge pumps with different C_p s. (b) Number of packets received on the gateway node with various C_p s.

$C1 - C3$ are connected in series. After that, the charge pump's voltage drops to 1.3V. Then, the power management module goes back to the charging mode. Overall, it takes the charge pump about 4 to 5 hours to be fully charged.

If a smaller supercapacitor $C_p = 50mF$ is used on the charge pump, we see that the charging times are significantly reduced in Figure 12(b). In this case, the charge pump will discharge every 2 to 3 hours. We note that the charging time is not a constant because it is affected by the aquatic environment where the MFC is located. We conduct the same tests for a week and discover the charge pump's performance is relatively stable.

6.1.1 Discharging Time. We know the value of C_p affects the charge pump's charging time; it also significantly changes the discharging time and the amount of data collected. In this experiment, we choose four supercapacitors: $C_p = 33mF$, $50mF$, $100mF$, and $200mF$.

As shown in Figure 13(a), the smaller the capacitance of C_p , the shorter the charging and discharging times are. When $C_p = 33mF$, the charge pump is fully charged in about 55 minutes (on average). Its discharging time is about 0.68s, which is just enough to collect and transmit one piece of temperature data. On the other hand, the power management module can power a sensor for 8 seconds if $C_p = 200mF$. In this case, however, the charging time is about 5 hours.

We extend the previous experiments by installing a temperature sensor and a DO sensor on the TelosB sensor. For each round of discharging (of the charge pump), various numbers of messages are sent by the TelosB sensor given different C_p s. As shown in Figure 13(b), when $C_p = 33mF$, the sensor only sends one message about temperature, due to the limited energy collected in C_p . When $C_p = 50mF$, the harvested energy in C_p allows the sensor to transmit one DO and two temperature data. When C_p is $100mF$, the number of messages about temperature and DO is increased to five and two, respectively. In the last case, where $C_p = 200mF$, we find that nine temperature and five DO data are collected.

Insights: In practice, a large C_p is preferred for two reasons. A large C_p allows a sensor to collect more types of data, and it is desirable for a water quality monitoring system. In addition, a large C_p provides a sensor the opportunity to retransmit lost data in a congested wireless environment. Nevertheless, the sample rate will be significantly reduced given a large C_p . This tradeoff issue is worthwhile for additional research, which is considered our future work.

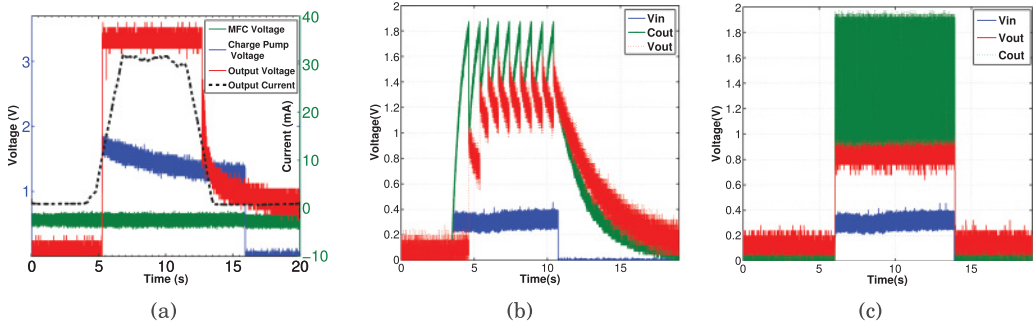


Fig. 14. (a) Instantaneous voltages and currents on the charge pump, the power management module, and the sensor when $C_p = 200\text{mF}$. (b) Instantaneous voltages of V_{in} , C_{out} , and V_{out} when $C_1 = C_2 = 1\mu\text{F}$. (c) Instantaneous voltages of V_{in} , C_{out} , and V_{out} when $C_1 = C_2 = 33\text{pF}$.

6.1.2 Instantaneous Voltage Measurement. We then investigate the instantaneous voltages and currents on the charge pump, the power management module, and the sensor. In Figure 14(a), we can see the MFC's voltage is around 0.33V . During the first 5 seconds, both the charge pump and the three supercapacitors are being charged. At the fifth second, the charge pump's voltage raises to 1.8V and it starts discharging. Right after that, the power management module's voltage increases to 3.3V (supercapacitors are connected in series). After about 8 seconds (with $C_p = 200\text{mF}$), the charge pump's voltage decreases to 1.3V , which is not sufficient to control switches. Therefore, the switches $S_1 - S_5$ are closed and the charge pump's voltage returns to 0. During these 8 seconds, the power management module's output voltage is around 3.3V ; the sensor draws various amount currents, at a maximum of 40mA .

6.2 RF Activation Module

Let the gateway node transmit 549MHz RF signals at 27dBm ; we evaluate the performance of the RF activation module in experiments. A dipole antenna, consisting of two 5.08-inch AWG magnetic copper wires, is installed on the RF activation module. Together with the sensor, the RF activation module is placed in a fixed location in the stream. We move the gateway node to various locations, so different distances between the gateway and sensor are obtained. When the distance increases, the voltage on V_{in} decreases. Once it is below 0.3V , the activation is ceased because the lowest operational voltage of the S-882Z chip is 0.3V . From experiments, we find the maximum activation distance is about 60 feet. In practice, the transmission power could be increased to 1dB , and the activation range could be longer than 60 feet.

Insights: To increase the activation distance and reduce the power consumption on the gateway node, a lower-frequency (540MHz) RF spectrum is adopted in the proposed system to remotely activate the sensors. This spectrum is located in the TV band and is widely used in RF energy-harvesting applications (Sample and Smith 2009). Meanwhile, this band will not cause interference to the Zigbee communications between sensors. We find that the proposed design on the RF antenna and the averaging stage, consisting of D_s diodes and corresponding capacitors, can efficiently harvest energy from the 540MHz radio signals. On one hand, we want to achieve a long activation range so that a large water area can be monitored. On the other hand, the gateway node powered by two 20W solar panels can only support 27dBm transmit power. A tradeoff issue exists here and needs further investigation, which is considered our future work. In the experiments, we find the maximum activation distance is about 60 feet.

There may be wireless interference in the proposed system; that is, the sensors are mistakenly activated by noise RF signals. In a regular scenario, however, we find the ambient RF signals are usually very weak (Liu et al. 2013; Kim et al. 2014; Xiao et al. 2015). The voltage threshold on V_{in} ensures that ambient noise RF radios will not activate sensors because the received signal strengths of a UHF radio are too weak to output 0.3V voltage to V_{in} . In some special cases, noise RF radios may activate the RF module if sensors are deployed close to a television transmitter. We do not consider this scenario because our system is usually deployed in a rural area. If sensors are deployed close to a TV tower or cellular base station, we could utilize the RF energy-harvesting technique, instead of MFCs, to power the sensors (Xiao et al. 2015).

6.2.1 Activation Delay. Because the RF activation module's performance is highly affected by C_1 and C_2 , we conduct experiments with $C_1 = C_2 = 1\mu\text{F}$ and $C_1 = C_2 = 33\text{pF}$, respectively. When large capacitors $C_1 = C_2 = 1\mu\text{F}$ are used, we record the instantaneous voltages of V_{in} , C_{out} , and V_{out} in Figure 14(b). The line about V_{in} gives the input voltage of received RF signals (at a 60-foot distance). The lines about C_{out} and V_{out} provide the voltages of C_1 and C_2 , respectively. At the third second, an RF signal is received, so V_{in} immediately raises to 0.3V. The supercapacitor C_1 is then charged and the C_{out} 's voltage increases. At the fourth second, C_{out} 's voltage reaches 1.8V and C_1 starts discharging. Because C_2 is charged, the V_{out} 's voltage equals C_2 's. As a result, the MOSFET switch is closed and the sensor is powered on. At the 11th second, as RF signals are not in present, C_1 discharges and C_{out} 's voltage decreases. That causes V_{out} 's voltage to decrease and the MOSFET switch to open at the 12th second.

An obvious delay is observed in Figure 14(b), where the sensor is activated 1 second after the RF signal is received. To address this issue, we select smaller capacitors $C_1 = C_2 = 33\text{pF}$. With this setting, an instantaneous activation is realized as shown in Figure 14(c). At the sixth second, the MOSFET switch is closed right after the activation RF signal is received. We note the voltages of V_{out} and C_{out} decrease to 0 immediately after the RF signal disappears. Compared to $C_1 = C_2 = 1\mu\text{F}$, the setting of $C_1 = C_2 = 33\text{pF}$ provides a better real-time performance. For this reason, we use $C_1 = C_2 = 33\text{pF}$ in our RF activation module.

Insights: Except for RF signals, other types of signals can also be used as the activation signals. For example, the headlight of a vehicle can be used to activate nodes in a traffic-monitoring sensor network. Acoustic signals emitted by a target could turn on sensors in a target-tracking sensor network (Lim et al. 2008; Chen et al. 2011).

6.2.2 Adjustable Working Periods. From Figure 14(a), we observe that the energy collected by MFC allows a sensor to work for 8 seconds when $C_p = 200\text{mF}$. To have a different working period, the sensor must have a different C_p in its power management circuit. Hardware changes on the power management circuit will be extremely difficult, if not impossible, after the system is deployed. On the other hand, if enough data are collected previously, it might be desirable for sensors to work for shorter periods of time to save the precious energy harvested by MFCs. To meet these goals, we can dynamically change the duration of the activation RF signals so that adjustable working periods on a sensor can be realized.

Within each round of activation, the gateway node periodically sends RF activation signals; that is, it sends RF signals for 400ms and stops for 400ms. As shown in Figure 15(a), the RF activation module's voltage periodically (every 400ms) switches between 1.8V and 0V. When the voltage is 1.8V, the MOSFET switch is closed and the power management module outputs 3.3V power to the sensor for 400ms, as shown in Figure 15(b). After that, RF signals disappear and the MOSFET switch is open. Because the charge pump stops discharging, its voltage decreases slightly (from 1.8V when it is in the discharging mode) for 400ms, as shown in Figure 15(c). From the figure, we can see the sensor is activated 18 times within 16 seconds; that is, it works for 400ms whenever

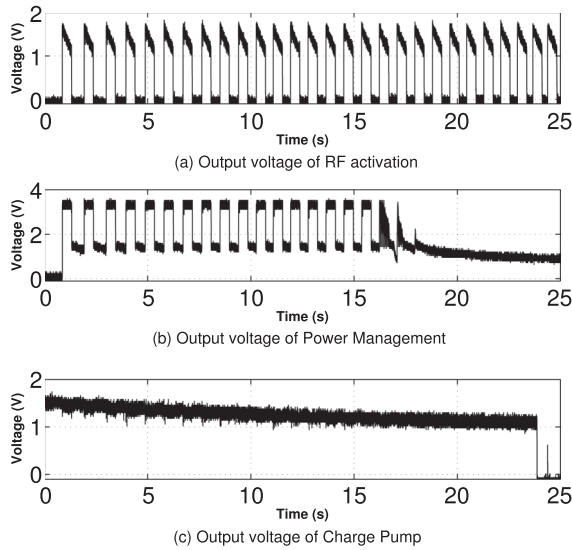


Fig. 15. Adjustable working periods can be realized on a sensor by changing the duration of RF activation signals.

it is activated. After the 16th second, the charge pump's voltage is too low to close the switches. Consequently, the sensor cannot be powered on. After the 23rd second, the power management module goes into the charging mode, and the charge pump's voltage becomes 0V. In this way, by adjusting the duration of RF signals, we are able to control how long a sensor works.

Insights: The proposed adjustable working periods on sensors can also be used for power management in the proposed system. For example, the gateway can send a short period of RF signals to activate sensors. Along with sensing data, a sensor also provides the gateway with its charge pump's voltage. Based on this information, the gateway obtains global knowledge on the energy level of the entire sensing system. It can leverage such information to determine the best time to activate sensors in the future.

6.3 System Deployment

The proposed sensing system, including two TelosB nodes, two temperature sensors, one DO sensor, one pH sensor and a gateway node, is tested in the same stream for more than 3 months. As shown in Figure 16, two sensors are immersed in the stream and the gateway is placed on the roof of a nearby building. On each sensor, the power management and RF activation modules are enclosed in a waterproof box. The size of the sensor prototype is about 5cm×5cm (not including the RF activation antenna). The supercapacitor C_p in the power management module is 200mF. We picked this value for reliability reasons; that is, it allows a sensor to send nine copies of temperature data and five copies of DO data once it is activated. It is possible to choose a smaller C_p (e.g., 33mF) for better real-time performance. Due to the time limitation, we do not conduct the experiments but expect to see similar results.

Insights: There are mainly two reasons for sensors floating on the water surface in the field test. First, the proposed system is designed to monitor the quality of shallow waters. Water information such as temperature, pH, and DO values may change more frequently in this area, compared to the deep-water areas. Another reason is to keep the corresponding cost as low as possible, to support

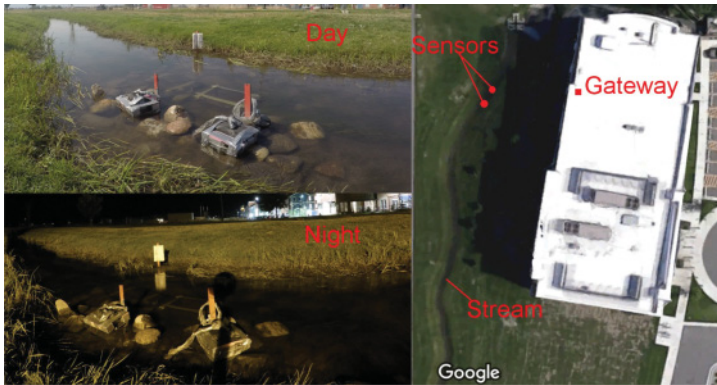


Fig. 16. Two sensors are deployed and tested in a local stream from July 20, 2015, to October 20, 2015.

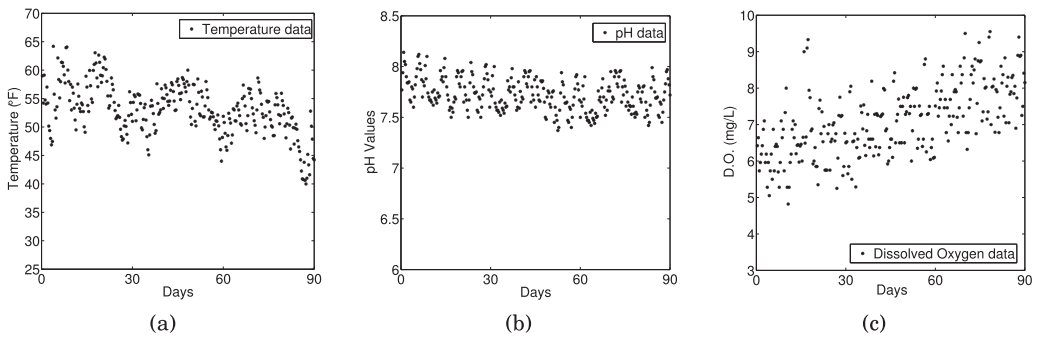


Fig. 17. (a) Temperature, (b) pH, and (c) dissolved oxygen data collected in a three-month field test.

large-scale deployment. This is because installing a watertight sensing system in an aqueous environment could be very challenging and expensive. In fact, the sensor and its power management module could be placed under the water as long as the wireless antenna part is above the water. With advanced waterproof packing techniques, it is possible to integrate acoustic communication modules into the sensors to replace the RF antennas, which is considered our future work. The major challenge of applying acoustic signals in transmit sensing data lies in acoustic communication modules usually consuming large amounts of energy. To address this issue, we may have to use a larger-size MFC or place the entire system in a marine environment.

6.4 Water Quality Monitoring

In the field test, one sensor collects temperature and pH data and the other one measures temperature and DO data. The data is currently stored on a local server; however, it could be saved on the cloud to achieve efficient and secure data query (Xia et al. 2016; Fu et al. 2016a; Liu et al. 2016). As shown in Figure 17, we received 2,079 SMS (Short Message Service) messages for temperature, 985 messages for pH, and 905 messages for DO data. We can clearly see that the temperature decreases gradually from July 2015 to October 2015. The fluctuation between adjacent data points generally reflects the temperature changes between day and night. From Figure 17(b), we find that cold water can hold more dissolved oxygen than warm water, which is reconcilable with common sense. On the other hand, it seems that the stream's pH value stays stable around 7.7 and does not change with temperatures, as shown in Figure 17(c). We also observe a total of 137 empty

packets, which might be caused by the interference between Zigbee and WiFi signals (in the building). The application of the proposed technology is not limited to water quality monitoring; in fact, it can also be used for water pollution detection, near-shore environment monitoring, and ocean oil pipeline monitoring.

Insights: Our system is designed to reliably collect accurate sensing data from sensors in the water. The achieved data rate can meet the need for regular water quality monitoring applications. In fact, it is better than the start-of-the-art solution that requires people to manually collect and analyze water samples. According to our design, it takes several hours for the power management module to cumulate enough energy generated from MFCs. This energy is enough to power a sensor for several seconds to collect sensing data from its probes and send data packages to the gateway node. With a shorter charging time, a higher data rate can be achieved; however, the time for collecting and sending data will be reduced. With a shorter working time, the collected data may be inaccurate because the readings from sensing probes are not stabilized. In addition, the data may be completely lost if there is not enough time for retransmissions. This tradeoff issue is worthwhile for additional research, which is considered our future work. In summary, our design is actually limited by the performance of MFC.

Lessons: We tried to place the gateway under a tree nearby the stream; however, it turns out to be a bad choice for two reasons. First, the non-light-of-sight (NLOS) between the gateway and sensors will affect not only data communication from sensors to the gateway but also the RF activation's efficiency. Second, the 20W solar panels do not always harvest enough solar energy to power the gateway. In the field tests, we also realized it is critical to put metal covers on the components immersed under the water because wildlife in the stream will bite them and cause severe system issues. We also discovered that it is impossible to read data from all sensing probes at the same time. That will cause a surge voltage consumption on the sensor, resulting in a system failure. We schedule the ADC and UART reading tasks on a sensor, so the high-volume instantaneous power consumption is avoided. Last but not the least, humidity will cause hardware failure. In the waterproof box, we placed a lot of desiccant to mitigate the humidity issue.

7 RELATED WORK

Energy-Harvesting Sensor Networks: Wireless sensor networks (Xie and Wang 2014; Chen et al. 2010; Du et al. 2007a) and underwater sensor networks (Han et al. 2015; Shen et al. 2015) have been widely studied in the last decade; however, there is a lack of empirical studies on energy-harvesting sensor networks in real-world aquatic environments. Powering a sensor network by renewable energy has drawn more and more attention recently, due to its potential to provide perpetual data services. To monitor the surrounding environment, the long-lived, self-sustained, and low-cost sensors can extract ambient energy from solar, heat, vibration, and RF radio (Kausar et al. 2014). For example, solar-powered sensor networks have been designed to improve data reliability (Yang et al. 2009; Wang et al. 2009 and Yang et al. 2010) and enable long-lived sensing systems (Lin et al. 2005). Leveraging thermoelectric harvesting, a low-power monitoring system for nonintrusive water flow detection, is proposed in Martin et al. (2012). By harvesting energy from the magnetic field radiating from AC power lines, a global clock synchronization can be achieved in sensor networks (Rowe et al. 2009). Making use of the energy from air flow introduced by a heating, ventilation, and air-conditioning (HVAC) system, Li et al. (2013) designed a self-sustaining indoor sensing system. To monitor surrounding environments, sensors can be powered by ambient energy harvested from RF radio, such as TV, cellular, and Wi-Fi signals (He et al. 2013; Kim et al. 2014; Fu et al. 2013). By using energy in ambient TV radios, the Ambient Backscatter system is able to power a sensor (Liu et al. 2013, Sample and Smith 2009). Similarly, it is demonstrated that Wi-Fi signals can be used to deliver power to low-power sensors and devices (Talla et al. 2015).

However, there are limitations on powering a sensor in the water using solar, heat, vibration, or radio.

Microbial Fuel Cells: To harvest energy from water, microbial fuel cells proved to be a promising solution, which allows bacteria to oxidize organic molecules and release electrons (Logan et al. 2006). The idea of extracting energy from microorganisms to produce electric current has been explored since the 1970s (Suzuki et al. 1978). It is well known that MFCs can survive for decades to generate electricity, using bacteria to break down organic substrates (Du et al. 2007b). Because MFCs typically produce power at a density of several *mW* per square meter, it was not considered in any practical usage (Liu and Logan 2004). However, recent research on MFCs has significantly enhanced the power output of MFCs and thus created renewed interest in applying MFCs in real-world applications (Rabaey et al. 2009). For instance, using bacteria living in water, MFCs can convert energy available in a bioconvertible substrate into electricity (Rabaey and Verstraete 2005). In a marine environment, sediment MFCs are used to harvest energy to power some marine devices (Hong et al. 2010). In this system, an electrode is placed into a marine sediment that is rich in organic matter. The other electrode is put above the water so that electricity can be generated. Installing such a system in an aqueous environment is challenging because the two electrodes are connected by a wire. The length of the wire must be at least equal to the depth of the water. Therefore, they are usually used in shallow sea areas. Unlike existing solutions, the proposed MFC features a biocathode coupled with a sacrificial anode, which does not require a cathode to be put in sediment nor an anode above the water.

Ultra-Low Power Management: Power management in energy-harvesting sensor networks has been widely studied. The importance of power management in energy-harvesting sensor networks was first discussed in Kansal et al. (2007). It was concluded that a sensor network powered by energy-harvesting techniques is fundamentally different from that powered by batteries. Paradiso and Starner (2005) introduced a few techniques for efficient power management, for example, dynamic optimization of a device's clock rate, hybrid analog-digital design, and smart duty-cycle mechanism. Similarly, Buchli et al. (2014) proposed to dynamically adjust the performance level of an energy-harvesting sensor network so that a long-term uninterrupted operation is achieved.

Looking at the same problem from a different angle, a charge pump is introduced to efficiently manage power harvested from ultra-low power sources in Meehan et al. (2011). To ensure discharged power is enough to power a sensor, it usually takes the charge pump (with a 2,200*mF* supercapacitor) a very long time to be fully charged. Instead of using a charge pump to accumulate energy, we propose to use it to control switches, so an efficient power management is achieved.

Recently, using harvested RF energy to power low-power-consumption devices has become very popular. For example, the WISP device can be powered by wireless signals sent from several meters away (Sample et al. 2008). Due to its low energy density, however, the energy from RF signals is not sufficient to power regular electronic devices (Nintanavongsa et al. 2012). In Ba et al. (2010), the harvested RF energy from WISP is used to wake up a Tmote Sky mote. Unlike existing works, we use harvested RF energy to control when and how long a sensor is connected to its power supply.

8 CONCLUSIONS

In this article, we explored the feasibility of building an MFC-powered and self-sustained water quality monitoring system. The visionary technology is designed, implemented, and tested in a real-world setting. From field tests, we concluded that the proposed system is effective, efficient, and robust. Each sensor in the deployed system is functional in collecting pH, dissolved oxygen concentration, and temperature data for a local stream. The innovation of the proposed system lies in the coupling of in situ remote monitoring of water quality with renewable and self-sustaining bioenergy generation. To make good use of the limited amount of harvested energy from MFCs,

an efficient power management system and a remote RF activation module are introduced. Experimental results indicate that we can realize on-demand activation and achieve synchronized communications between sensors in the system.

We anticipate a much better performance of the MFC once it is implemented in a marine environment where the electric conductance of seawater is much greater than that seen in streams, leading to much lower internal resistance of the MFC. The seawater features an electrical conductivity at least 100 times as high as that of stream water (5 vs. 0.05S/m). One can expect the power output of MFCs to be 100 times higher in seawater than in stream water. Note that MOMs are abundant in both freshwater and sea aquatic environments. Because Zigbee signals do not penetrate water, it is essential to integrate an acoustic communication module into the sensor in the future. The challenge of using acoustic signals to transmit sensing data is that acoustic communication modules consume large amounts of energy. This problem becomes even more challenging given the limited amount of energy harvested by MFCs.

REFERENCES

- Ala Al-Fuqaha, Mohsen Guizani, Mehdi Mohammadi, Mohammed Aledhari, and Moussa Ayyash. 2015. Internet of things: A survey on enabling technologies, protocols, and applications. *IEEE Communications Surveys & Tutorials* 17, 4 (2015), 2347–2376.
- He Ba, Ilker Demirkol, and Wendi Heinzelman. 2010. Feasibility and benefits of passive RFID wake-up radios for wireless sensor networks. In *2010 IEEE Global Telecommunications Conference (GLOBECOM'10)*. IEEE, 1–5.
- Bernhard Buchli, Felix Sutton, Jan Beutel, and Lothar Thiele. 2014. Dynamic power management for long-term energy neutral operation of solar energy harvesting systems. In *Proceedings of the 12th ACM Conference on Embedded Network Sensor Systems*. ACM, 31–45.
- Jiming Chen, Kejie Cao, Keyong Li, and Youxian Sun. 2011. Distributed sensor activation algorithm for target tracking with binary sensor networks. *Cluster Computing* 14, 1 (2011), 55–64.
- Jiming Chen, Weiqiang Xu, Shibo He, Youxian Sun, Preetha Thulasiraman, and Xuemin Shen. 2010. Utility-based asynchronous flow control algorithm for wireless sensor networks. *IEEE Journal on Selected Areas in Communications* 28, 7 (2010), 1116–1126.
- Xiaojiang Du, Mohsen Guizani, Yang Xiao, and Hsiao-Hwa Chen. 2007a. Two tier secure routing protocol for heterogeneous sensor networks. *IEEE Transactions on Wireless Communications* 6, 9 (2007), 3395–3401.
- Zhuwei Du, Haoran Li, and Tingyue Gu. 2007b. A state of the art review on microbial fuel cells: A promising technology for wastewater treatment and bioenergy. *Biotechnology Advances* 25, 5 (2007), 464–482.
- Lingkun Fu, Peng Cheng, Yu Gu, Jiming Chen, and Tian He. 2013. Minimizing charging delay in wireless rechargeable sensor networks. In *Proceedings of the 32nd IEEE International Conference on Computer Communications*. 2922–2930.
- Zhangjie Fu, Fengxiao Huang, Xingming Sun, Athanasios Vasilakos, and Ching-Nung Yang. 2016a. Enabling semantic search based on conceptual graphs over encrypted outsourced data. *IEEE Transactions on Services Computing* PP, 99 (2016).
- Zhangjie Fu, Xingming Sun, Sai Ji, and Guowu Xie. 2016b. Towards efficient content-aware search over encrypted outsourced data in cloud. In *Proceedings of the 35th Annual IEEE International Conference on Computer Communications (IEEE INFOCOM'16)*. IEEE, 1–9.
- Omprakash Gnawali, Rodrigo Fonseca, Kyle Jamieson, David Moss, and Philip Levis. 2009. Collection tree protocol. In *Proceedings of the 7th ACM Conference on Embedded Networked Sensor Systems*. ACM, 1–14.
- Yu Gu and Tian He. 2007. Data forwarding in extremely low duty-cycle sensor networks with unreliable communication links. In *Proceedings of the 5th International Conference on Embedded Networked Sensor Systems (SenSys'07)*. ACM, New York, 321–334. DOI : <http://dx.doi.org/10.1145/1322263.1322294>
- Guangjie Han, Jinfang Jiang, Na Bao, Liangtian Wan, and Mohsen Guizani. 2015. Routing protocols for underwater wireless sensor networks. *IEEE Communications Magazine* 53, 11 (2015), 72–78.
- Shibo He, Jiming Chen, Fachang Jiang, David K. Y. Yau, Guoliang Xing, and Youxian Sun. 2013. Energy provisioning in wireless rechargeable sensor networks. *IEEE Transactions on Mobile Computing* 12, 10 (2013), 1931–1942.
- Shibo He, Jiming Chen, and Youxian Sun. 2012. Coverage and connectivity in duty-cycled wireless sensor networks for event monitoring. *IEEE Transactions on Parallel and Distributed Systems* 23, 3 (2012), 475–482.
- Seok Won Hong, Han S. Kim, and Tai Hak Chung. 2010. Alteration of sediment organic matter in sediment microbial fuel cells. *Environmental Pollution* 158, 1 (2010), 185–191.

- Xiaofan Jiang, Joseph Polastre, and David Culler. 2005. Perpetual environmentally powered sensor networks. In *4th International Symposium on Information Processing in Sensor Networks, 2005 (IPSN'05)*. IEEE, 463–468.
- Aman Kansal, Jason Hsu, Sadaf Zahedi, and Mani B. Srivastava. 2007. Power management in energy harvesting sensor networks. *ACM Transactions on Embedded Computing Systems (TECS)* 6, 4 (2007), 32.
- A.S.M. Zahid Kausar, Ahmed Wasif Reza, Mashad Uddin Saleh, and Harikrishnan Ramiah. 2014. Energizing wireless sensor networks by energy harvesting systems: Scopes, challenges and approaches. *Renewable and Sustainable Energy Reviews* 38 (October 2014).
- Sangkil Kim, Rushi Vyas, Jo Bitto, Kyriaki Niotaki, Ana Collado, Apostolos Georgiadis, and Manos M. Tentzeris. 2014. Ambient RF energy-harvesting technologies for self-sustainable standalone wireless sensor platforms. *Proceedings of the IEEE* 102, 11 (2014), 1469–1666.
- Alvin Lim, Qing Yang, Kenan Casey, and Raghu-kisore Neeliseti. 2008. Real-time target tracking with CPA algorithm in wireless sensor networks. In *Proceedings of the 5th Annual IEEE Communications Society Conference on Sensor, Mesh and Ad Hoc Communications and Networks, 2008 (SECON'08)*. IEEE, 305–313.
- Kris Lin, Jennifer Yu, Jason Hsu, Sadaf Zahedi, David Lee, Jonathan Friedman, Aman Kansal, Vijay Raghunathan, and Mani Srivastava. 2005. Heliomote: Enabling long-lived sensor networks through solar energy harvesting. In *Embedded Networked Sensor Systems*. 309–309.
- Hong Liu and Bruce E. Logan. 2004. Electricity generation using an air-cathode single chamber microbial fuel cell in the presence and absence of a proton exchange membrane. *Environmental Science & Technology* 38, 14 (2004), 4040–4046.
- Qi Liu, Weidong Cai, Jian Shen, Zhangjie Fu, Xiaodong Liu, and Nigel Linge. 2016. A speculative approach to spatial-temporal efficiency with multi-objective optimization in a heterogeneous cloud environment. *Security and Communication Networks* 9, 17 (2016), 4002–4012.
- Vincent Liu, Aaron Parks, Vamsi Talla, Shyamnath Gollakota, David Wetherall, and Joshua R. Smith. 2013. Ambient backscatter: Wireless communication out of thin air. In *Proceedings of the ACM SIGCOMM 2013 Conference on SIGCOMM (SIGCOMM'13)*. 39–50.
- Bruce E. Logan, Bert Hamelers, René Rozendal, Uwe Schröder, Jürg Keller, Stefano Freguia, Peter Aelterman, Willy Verstraete, and Korneel Rabaey. 2006. Microbial fuel cells: Methodology and technology. *Environmental Science & Technology* 40, 17 (2006), 5181–5192.
- MEMSIC. 2015. TelosB. http://www.memsic.com/userfiles/files/Datasheets/WSN/telosb_datasheet.pdf. (2015). [Online; accessed 02-April-2015].
- Paul Martin, Zainul Charbiwala, and Mani Srivastava. 2012. DoubleDip: Leveraging thermoelectric harvesting for low power monitoring of sporadic water use. In *Proceedings of the 10th ACM Conference on Embedded Network Sensor Systems (SenSys'12)*. ACM, New York, 225–238. DOI : <http://dx.doi.org/10.1145/2426656.2426679>
- Andrew Meehan, Hongwei Gao, and Zbigniew Lewandowski. 2011. Energy harvesting with microbial fuel cell and power management system. *IEEE Transactions on Power Electronics* 26, 1 (2011), 176–181.
- David Moss and Philip Levis. 2008. *BoX-MACs: Exploiting Physical and Link Layer Boundaries in Low-Power Networking*. Computer Systems Laboratory Stanford University, 116–119.
- Tuan Anh Nguyen, Yuzhuo Lu, Xinghong Yang, and Xianming Shi. 2007. Carbon and steel surfaces modified by *Leptothrix discophora* SP-6: Characterization and implications. *Environmental Science & Technology* 41, 23 (October 2007), 7987–7996.
- Prusayon Nintanavongsa, Ufuk Muncuk, David Richard Lewis, and Kaushik Roy Chowdhury. 2012. Design optimization and implementation for RF energy harvesting circuits. *IEEE Journal on Emerging and Selected Topics in Circuits and Systems* 2, 1 (2012), 24–33.
- J. A. Paradiso and T. Starner. 2005. Energy scavenging for mobile and wireless electronics. *Pervasive Computing* 4, 1 (2005), 18–27.
- Sebastian Pobering and Norbert Schwesinger. 2008. Power supply for wireless sensor systems. In *Proceedings of the 2008 IEEE Sensors*. 685–688.
- Anuradha Pughat and Vidushi Sharma. 2016. Performance analysis of an improved dynamic power management model in wireless sensor node. *Digital Communications and Networks* 3, 1 (2016), 19–29.
- Korneel Rabaey, Largus Angenent, Uwe Schröder, and Jürg Keller. 2009. Bioelectrochemical systems: From extracellular electron transfer to biotechnological application. IWA publishing.
- Korneel Rabaey and Willy Verstraete. 2005. Microbial fuel cells: Novel biotechnology for energy generation. *TRENDS in Biotechnology* 23, 6 (June 2005), 291–298.
- Theodore S. Rappaport. 1996. *Wireless Communications: Principles and Practice*. Prentice-Hall, Englewood Cliffs, NJ.
- Anthony Rowe, Vikram Gupta, and Rangunathan Raj Rajkumar. 2009. Low-power clock synchronization using electromagnetic energy radiating from ac power lines. In *Proceedings of the 7th ACM Conference on Embedded Networked Sensor Systems*. ACM, 211–224.

- Alanson Sample and Joshua R. Smith. 2009. Experimental results with two wireless power transfer systems. In *Proceedings of the IEEE Radio and Wireless Symposium*, 16–18.
- Alanson P. Sample, Daniel J. Yeager, Pauline S. Powledge, Alexander V. Mamishev, and Joshua R. Smith. 2008. Design of an RFID-based battery-free programmable sensing platform. *IEEE Transactions on Instrumentation and Measurement* 57, 11 (2008), 2608–2615.
- Jian Shen, Hao-Wen Tan, Jin Wang, Jin-Wei Wang, and Sung-Young Lee. 2015. A novel routing protocol providing good transmission reliability in underwater sensor networks. *Journal of Internet Technology* 16, 1 (2015), 171–178.
- Sujesha Sudevalayam and Purushottam Kulkarni. 2011. Energy harvesting sensor nodes: Survey and implications. *IEEE Communications Surveys & Tutorials* 13, 3 (2011), 443–461.
- Shuichi Suzuki, Isao Karube, and Tadashi Matsunaga. 1978. Application of a biochemical fuel cell to wastewaters. In *Biotechnology and Bioengineering Symposium*, Vol. 8. Tokyo Institute of Technology, Yokohama, Japan.
- Vamsi Talla, Bryce Kellogg, Benjamin Ransford, Saman Naderiparizi, Shyamnath Gollakota, and Joshua R. Smith. 2015. Powering the next billion devices with wi-fi. In *Proceedings of the 11th ACM Conference on Emerging Networking Experiments and Technologies (CoNEXT'15)*. 1–13.
- Bradley M. Tebo, Hope A. Johnson, James K. McCarthy, and Alexis S. Templeton. 2005. Geomicrobiology of manganese (II) oxidation. *TRENDS in Microbiology* 13, 9 (2005), 421–428.
- Preetha Thulasiraman and Kevin A. White. 2016. Topology control of tactical wireless sensor networks using energy efficient zone routing. *Digital Communications and Networks* 2, 1 (2016), 1–14.
- Lili Wang, Yong Yang, Dong Kun Noh, Hieu K. Le, Jie Liu, Tarek F. Abdelzaher, and Michael Ward. 2009. AdaptSens: An adaptive data collection and storage service for solar-powered sensor networks. In *Proceedings of the 30th IEEE Real-Time Systems Symposium, 2009 (RTSS'09)*. 303–312.
- Zhihua Xia, Xinhui Wang, Xingming Sun, and Qian Wang. 2016. A secure and dynamic multi-keyword ranked search scheme over encrypted cloud data. *IEEE Transactions on Parallel and Distributed Systems* 27, 2 (2016), 340–352.
- Tianyu Xiang, Zicheng Chi, Feng Li, Jun Luo, Lihua Tang, Liya Zhao, and Yaowen Yang. 2013. Powering indoor sensing with airflows: A trinity of energy harvesting, synchronous duty-cycling, and sensing. In *Proceedings of the 11th ACM Conference on Embedded Networked Sensor Systems (SenSys'13)*. 16:1–16:14.
- Lu Xiao, Ping Wang, Dusit Niyato, Dong In Kim, and Zhu Han. 2015. Wireless networks with RF energy harvesting: A contemporary survey. *IEEE Communications Surveys and Tutorials* 17, 2 (2015), 757–789.
- Shengdong Xie and Yuxiang Wang. 2014. Construction of tree network with limited delivery latency in homogeneous wireless sensor networks. *Wireless Personal Communications* 78, 1 (2014), 231–246.
- Yong Yang, Lu Su, Yan Gao, and Tarek F. Abdelzaher. 2010. SolarCode: Utilizing erasure codes for reliable data delivery in solar-powered wireless sensor networks. In *Proceedings of the 29th Conference on Computer Communications*. 1–5.
- Yong Yang, Lili Wang, Dong Kun Noh, Hieu Khac Le, and Tarek F. Abdelzaher. 2009. SolarStore: Enhancing data reliability in solar-powered storage-centric sensor networks. In *Proceedings of the 7th International Conference on Mobile Systems, Applications, and Services (MobiSys'09)*. ACM, New York, 333–346. DOI: <http://dx.doi.org/10.1145/1555816.1555850>
- Fu Zhangjie, Sun Xingming, Liu Qi, Zhou Lu, and Shu Jiangang. 2015. Achieving efficient cloud search services: Multi-keyword ranked search over encrypted cloud data supporting parallel computing. *IEEE Transactions on Communications* 98, 1 (2015), 190–200.

Received July 2016; accepted January 2017